J Mater Sci (2007) 42:3724–3731
DOI 10.1007/s10853-006-0378-z

Volume relaxation in amorphous and semicrystalline PET

Jiří Hadač · Petr Slobodian · Petr Sáha

Received: 5 September 2005 / Accepted: 28 April 2006 / Published online: 10 February 2007

Abstract Two types of polyethyleneterephthalate (PET) were investigated, one nearly amorphous and the other highly crystallized. DSC analysis and mercury-in-glass dilatometry were used to determine the effect of crystalline phase content on the thermal behavior of amorphous phase. Increasing portion of crystals caused an increase in glass transition temperature (T_g) and broadening of the transition zone. Thermal expansion coefficient and specific heat decreased. The amount of rigid amorphous fraction, RAF, was calculated to be around 21–26%. Volume relaxation measurements initiated by temperature down-jump from the equilibrium above T_g to several temperatures in the vicinity of T_g showed considerably reduced relaxation rate for semicrystalline PET.

Introduction

When amorphous polymers are cooled from liquid state above the glass transition temperature, T_g, to the temperatures below T_g, they are in thermodynamically non-equilibrium state. This can be proved by measurements of various material properties dependent on time under isothermal conditions. More precisely, in the case of quantities such as volume or enthalpy, one can easily observe their continuous decrease and for the temperatures within the region of glass transition temperature also a tendency to achieve the equilibrium values in reasonable experimental times [1–11]. This phenomenon is usually called structural relaxation or physical aging and appears with amorphous materials as well as with amorphous parts of semicrystalline polymers [5–15].

One of such semicrystalline polymers with common use is poly(ethylene terephthalate), PET. The poly(ethylene terephthalate) can be easily obtained in either amorphous or semicrystalline form, in a wide range of crystallinity as a result of thermal treatment in the temperature region between the glass transition temperature and melting temperature [6,8,11].

Semicrystalline PET generally consists of two phases with different structures and properties. One of them (crystalline phase) is formed into lamellas further associated into more superior objects, such as spherulites. The other phase is amorphous, represented by disordered molecules or their parts. Furthermore, the amorphous phase is not usually uniform and two distinct amorphous phases in semicrystalline PET with different thermal properties or relaxation kinetics can be revealed by some experimental techniques such as dielectric spectroscopy [12], dynamics mechanical experiments [13] or differential scanning calorimetry, DSC [7,8]. In the case of the DSC measurements, thermograms measured during heating of low-crystallinity samples, previously annealed at temperatures in the range of glass transition, show two transition peaks corresponding to two different types of amorphous regions [8,16,17]. One type of amorphous phase situated far enough from crystals retains the properties of pure or bulk amorphous polymer, mobile amorphous fraction, MAF, and the other type, in the vicinity of crystals, has consequently restricted conformational mobility of polymer chains,

J. Hadač (✉) · P. Slobodian · P. Sáha
Faculty of Technology, Polymer Centre, Tomas Bata University, T.G.M. 275, 762 72 Zlín, Czech Republic
e-mail: hadac@ft.utb.cz

rigid amorphous fraction, RAF. The former one is probably mainly situated outside of the spherulitic structure (interspherulitic amorphous regions), while the latter one constitutes the amorphous phase inside the spherulites (intraspherulitic amorphous regions) [6–8,11]. The two peaks measured by DSC represent the glass transformation of both amorphous modifications, one appearing at the lower temperature corresponding to the MAF, while the peak appearing at the higher temperature belongs to the RAF situated at the interface of both phases. In the case of highly crystalline PET, the amorphous phase will be principally located inside spherulites [7] and only the higher transition peak will be detected. The thickness of RAF is usually reported to be about 2–4 nm [16,17]. Its volume portion increases with the crystallinity and levels off at 25% of crystallinity [16,17].

Alves et al. [8] presented glass transition temperatures for amorphous PET, *a*-PET, and highly crystalline (semicrystalline) PET, *s*-PET. They found the transition temperatures to be 65 °C for *a*-PET and 92 °C for *s*-PET. However, it was found to be very difficult to characterize the glass transition temperature of semicrystalline PET accurately because the transition became less apparent and T_g region covered the range as wide as 70–110 °C [7,8]. This shift of glass transition temperature towards the higher values together with the broadening of the transition zone was frequently described and explained as the effect of crystals onto bulk thermal properties of the amorphous part of the material [5–11]. Further, the change in specific heat, Δc_p, associated with the transition, was reduced from the value around 0.33–0.41 J g^{-1} K^{-1} for *a*-PET [8,11,16–19] to 0.12–0.17 J g^{-1} K^{-1} for *s*-PET [7,16,17]. The changes observed in Δc_p with crystallinity were larger than that predicted by the two-phase model and this fact could be attributed to the presence of rigid amorphous phase [11,16,17].

The effect of crystallinity on structural relaxation has been reported in the literature by various researchers. Tant and Wilkes [20] evaluated the relaxation of semicrystalline PET films, and reported that the extent and rate of aging decreased with the increasing crystallinity. Calorimetric measurements of Alves et al. [8], Aref-Azar et al. [11] and Mukherjee and Jabarin [21] showed similar findings such as reduction in the extent and rate of enthalpy relaxation. Observation of Struik in amorphous [22] and semicrystalline [9,10] PET showed also considerable decrease in volume relaxation rate in large temperature range for the PET containing crystalline phase. Surprisingly, Itoyama [23] reported an opposite trend and the volume relaxation rate was found to increase at the low crystallinity content (3%) in comparison to pure amorphous PET. Chung et al. [24] reported similar findings during the study on starches containing different degrees of crystallinity. Observed increase in enthalpy relaxation rate with crystallinity was attributed to the differences in the sample preparation.

In this paper thermal analysis and volume relaxation measurements of PET with two degree of crystallinity was carried out. The amount of RAF was determined and its influence onto thermal and volume relaxation behavior was tested. Finally, volume-temperature dependences during sample heating through glass transition region were measured. This method represents non-isothermal measurement of structural relaxation, very rarely experimentally done in volume although DSC methodology is based on it.

Experimental

Material

Poly(ethylene terephthalate), PET, acquired from Aldrich Chemical Company was used in the experiments. From the original granules, two samples with different levels of crystallinity were prepared. The first sample composing of nearly amorphous PET is hereafter referred to as *a*-PET. The second sample representing a highly crystallized PET was denoted as *s*-PET. *a*-PET was prepared by pouring the melted polymer into room-temperature water contrary to *s*-PET which was prepared by slow cooling of melt with a rate of 2 °C min^{-1}. The densities were determined to be $\rho_a = 1{,}339.1 \pm 0.3$ kg m^{-3} and $\rho_s = 1{,}394.3 \pm 0.3$ kg m^{-3} for *a*-PET and for *s*-PET, respectively. Comparing these values with density of pure amorphous PET, $\rho_{am} = 1{,}335$ kg m^{-3} and with theoretical density of crystalline phase, $\rho_c = 1{,}501$ kg m^{-3} [25], the degree of crystallinity can be calculated as the weight fraction, w, or volume fraction, φ, Eqs. (1) and (2).

$$w = \frac{\rho_c}{\rho_{a,s}} \frac{(\rho_{a,s} - \rho_{am})}{(\rho_c - \rho_{am})} \tag{1}$$

$$\varphi = \frac{\rho_{a,s} - \rho_{am}}{\rho_c - \rho_{am}} \tag{2}$$

Wide-angle X-ray scattering

Independent determination of samples crystallinity was carried out using a wide-angle X-ray diffraction (HZG

4 Diffractometer). The X-ray diffractometer was equipped with CuK_α radiation (wavelength $\alpha = 0.154$ nm). Samples in the form of powder were scanned in the 2Θ from 5° to 60° in reflection mode using a step of 0.05 and the counting time of one scan of 5 s. The portion of crystalline phase, x_c, was calculated with the help of Eq. (3):

$$x_c = \frac{I_c}{I} \tag{3}$$

where I is total integral intensity of X-ray diffractogram and I_c is the integral intensity diffracted by crystalline part.

Thermal analyses

The thermal analyses of the samples were performed by calorimetric and dilatometric measurements.

For calorimetric measurements, DSC 1 Pyris (Perkin Elmer Inc.) was used. The temperature dependence of specific heat, c_p, was measured using sapphire standard at a cooling rate of 10 °C min^{-1}. Glass transition temperatures were determined as a half-c_p value.

Dilatometric data were obtained as volumetric one with the help of Mercury-in-Glass Dilatometry prepared according to ASTM Standard D 864-52. The dilatometers were filled with pure mercury, 99.9998%, under vacuum of about 2 Pa. The capillary bore of the diameters were 0.801 mm in the case of *a*-PET and 0.651 mm for *s*-PET. The amounts of both materials placed inside the dilatometers were 1.714 and 2.104 cm^3, respectively. Thermal programs were done by immersing the dilatometers into precisely programmable thermostatic bath Julabo HP 4 with the thermal stability ±0.02 °C (reported by the producer). The dependencies of specific volume on the temperature were measured during both cooling and heating at the same rate of 1 °C min^{-1} using a temperature ramp of the bath. Furthermore, in the cooling experiments, the initial temperature of T_i was chosen to be $T_i = T_{g,vol} + 18$ °C, in order to erase any previous thermal history of the specimens, and the dilatometer was maintained at this temperature for 15 min. In the heating experiments, a three-step procedure was applied. The dilatometer was cooled from $T_i = T_{g,vol} + 18$ °C, the cooling rate of 1 °C min^{-1}, to an annealing temperature, $T_a = T_{g,vol}$–15 °C, where the dilatometer was allowed to consolidate for some period of time, T_a, before final heating scan through the T_g region, at the rate of 1 °C min^{-1}, was done. The times, t_a, were 96 and 960 h for *a*-PET and 96 and 930 h for *s*-PET, respectively.

Volume relaxation measurements

The volume relaxation experiments were performed as temperature down-jumps from equilibrium state well above T_g to relaxation (consolidation) temperature, T_a, situated in T_g region followed by an isothermal stage. The annealing temperature was $T_i = T_g + 10$ °C was maintained for 20 min, and then, the temperature jumps were realized by a manual transfer of dilatometers from Julabo HP 4 to another precise thermostatic bath (Grant 14 with the thermal stability of ±0.004 °C, as reported by the producer). Zero time for collecting the relaxation data was set at 120 s after temperature jump The relaxation temperatures were chosen as follows: 69, 67, 65, 63, 61, 52 °C for *a*-PET and 83.1, 81.5, 80, 77, 75, 65 °C for *s*-PET. The materials were allowed to relax till equilibrium or for *s*-PET up to 200 h at $T_a = 77$ and 75 °C, but the equilibrium was not achieved. Two long-terms tests were performed for *a*-PET at 52 °C, and for *s*-PET at 65 °C, in which the relaxation time was extended beyond 504 h.

Cold crystallization

The dilatomether with *a*-PET was maintained at 106 °C for 10 and next 8 min to increase crystalline content determined to be 4.2 and 7.0 wt.%, respectively. V–T dependences were measured during cooling of 1 °C min^{-1}. T_g'*s* and thermal expansion coefficients of both new compositions were calculated.

Results and discussion

Overall, any thermal treatment of crystallizable polymer like PET, can cause change in its crystalline content or cause other changes in crystalline structure (recrystallization). For this reason, thermal analysis to find safe annealing temperature where crystallization does not occur in the timescales of cooling/heating cycles or annealing before temperature down-jump to relaxation temperature were performed. This temperature for amorphous PET was chosen to be around 95 °C. Here, after approximately 10 h no volume changes representing volume contraction of possible crystallization were detected. This temperature was chosen as a maximum in the case of heating/cooling scans. The annealing temperature before temperature down-jump was chosen even lower. The reason was to

lower temperature jump and consequently to reach shorter time of temperature equalization inside of the dilatometer.

According density measurements, weight and volume content of crystalline phase were calculated by Eqs. (1) and (2). For the *a*-PET, the values are $w_a = 2.8$ wt.% and $\varphi_a = 2.5$ vol.%, and for *s*-PET $w_c = 42.6$ wt.% and $\varphi_c = 39.8$ vol.%.

Determination of sample crystallinity by X-ray scattering was done with help of Eq. (3). Figure 1 displays X-ray diffractograms of *a*-PET (lower) and *s*-PET (upper). The measurements of *a*-PET shows a wide band, characteristic of a non-crystalline material, tiny peaks points to the residual degree of crystallinity. The calculation gives 2.1% of crystallinity. On the upper diffractogram sharp diffraction peaks gives value of 37.4%. Both density and X-ray scattering methods give comparable insight into state of PET crystallinity.

Figure 2 shows the temperature dependence of specific heat, c_p, for both investigated materials measured at the cooling rate of 10 °C min^{-1}. The content of crystalline phase decreases c_p in both temperature regions, above and below T_g. The difference in c_p in the glass transition region can be determined as, $\Delta c_p = c_{pl} - c_{pg}$, where c_{pg} is specific heat for the glassy state and c_{pl} for the liquid state. Δc_p achieve values 0.35 J g^{-1} K^{-1} for *a*-PET and 0.15 J g^{-1} K^{-1} for *s*-PET (Table 1). The glass transition temperature (as a half-c_p value) was determined to be 69.1 °C for *a*-PET and 81.5 °C for *s*-PET, some 12.4 °C shift of T_g caused by crystallinity was found.

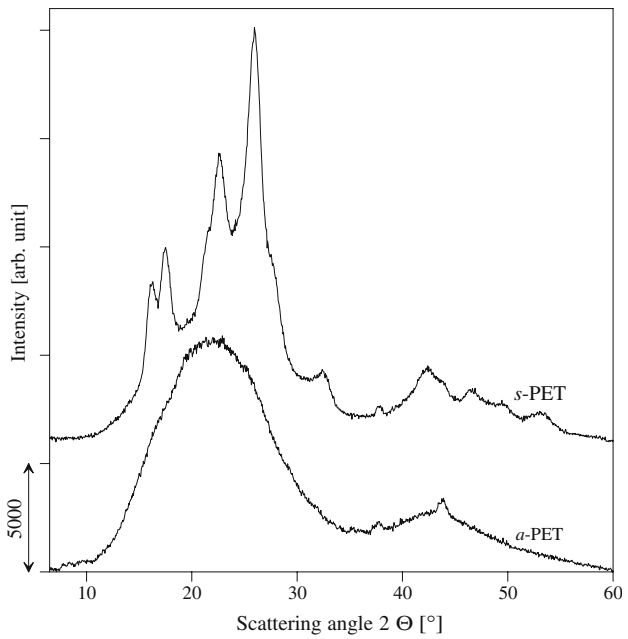

Fig. 1 X-ray diffractograms for *a*-PET and *s*-PET

Volume-temperature dependencies during sample cooling and heating are presented in Fig. 3 a, b. The glass transition temperature can be evaluated as an intersection of equilibrium liquid line with asymptotic glassy line, giving the value of $T_g = 67.8$ °C for *a*-PET and 77.5 °C for *s*-PET, Table 1. Thus, the crystalline phase shifts T_g of the amorphous part of *s*-PET some 9.7 °C to higher temperature compared to *a*-PET. Also broadening of the transition zone can be seen.

The parts of Fig. 3 a, b further contain heating scans of consolidated samples. The situation during specimens heating differs in the shape of V–T curves and also position of T_g region is shifted to higher temperatures compared with cooling. A typical abrupt change is found in the temperature dependence of volume in the T_g region. The volume expands following a slope of glassy state through equilibrium liquid line (dashed line in Fig. 3a) and after some temperature overheating it the volume changes nearly steeply achieving equilibrium melt. This change is increased and shifted to higher temperatures by the time of consolidation below T_g, which can be documented for both *a*-PET and *s*-PET.

From the cooling and heating scans the temperature dependence of thermal expansion coefficient can be calculated, as presented in Fig. 3c and d. From the cooling data one achieves a step change in T_g. From the heating data, peaks in thermal expansion coefficients are calculated, which are analogical to peaks in heat flow usually determined by calorimetric measurements on DSC apparatus [1,2,6–8]. The area of these peaks increases and their maximum is shifted to higher temperatures with the time of consolidation below T_g. The content of crystalline phase significantly decreases the height and the area of such transition peaks; see different scales of thermal expansion coefficient coordinates, Fig. 3c, d. Single peak in $\alpha(T)$ *s*-PET dependency after 930 h of annealing indicate the presence of only one type of amorphous phase.

The calculated thermal expansion coefficients above and below T_g are presented in Table 1. In both cases they are lowered by specimen crystallinity. Also the difference in thermal expansion coefficients between liquid and glass, $\Delta\alpha = \alpha_l - \alpha_g$, where α_l is thermal expansion coefficients in liquid and α_g in glass is reduced by the presence of crystalline phase from 3.31×10^{-4} K^{-1} for *a*-PET to 1.27×10^{-4} K^{-1} for *s*-PET.

Following the original work of Wunderlich et al. [26,27] the weight portion of the rigid amorphous fraction, x_w, can be calculated as:

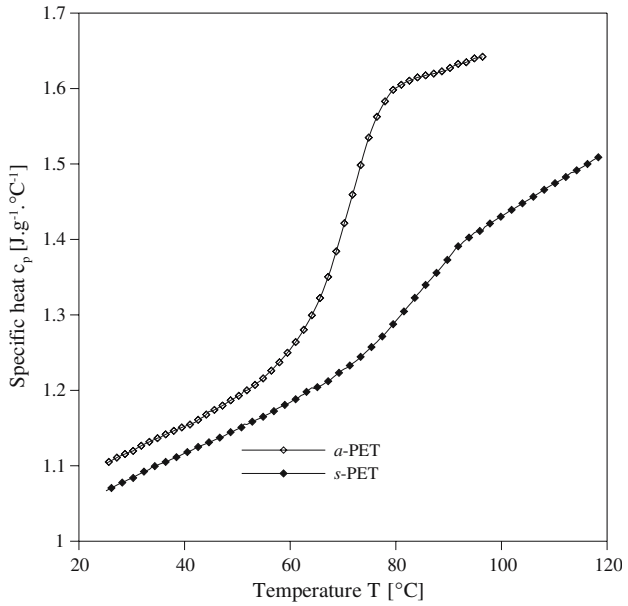

Fig. 2 Temperature dependence of specific heat for *a*-PET and *s*-PET measured by cooling rate 10 °C min^{-1}

$$x_w = \left(1 - \frac{\Delta c_{ps}}{\Delta c_{pam}} - w_c\right) \quad (4)$$

where Δc_p represents the difference in specific heat between liquid and glass, subscript am stands for amorphous phase and s for tested samples, w_c represents the above calculated degree of crystallinity by weight. In order to determine the amounts of RAF from calorimetric data, a value of Δc_p of 0.41 J g^{-1} K^{-1} [18,19] was adapted for fully amorphous sample, and the results are summarized in Table 1.

Equation (5) can also be adapted for the data from volume measurements:

$$x_\varphi = \left(1 - \frac{\Delta \alpha_s}{\Delta \alpha_{am}} - \varphi_c\right) \quad (5)$$

where $\Delta\alpha$ is the difference in thermal expansion coefficient between liquid and glass, and φ_c is the degree of crystallinity calculated as the volume fraction. The difference in thermal expansion coeffi-

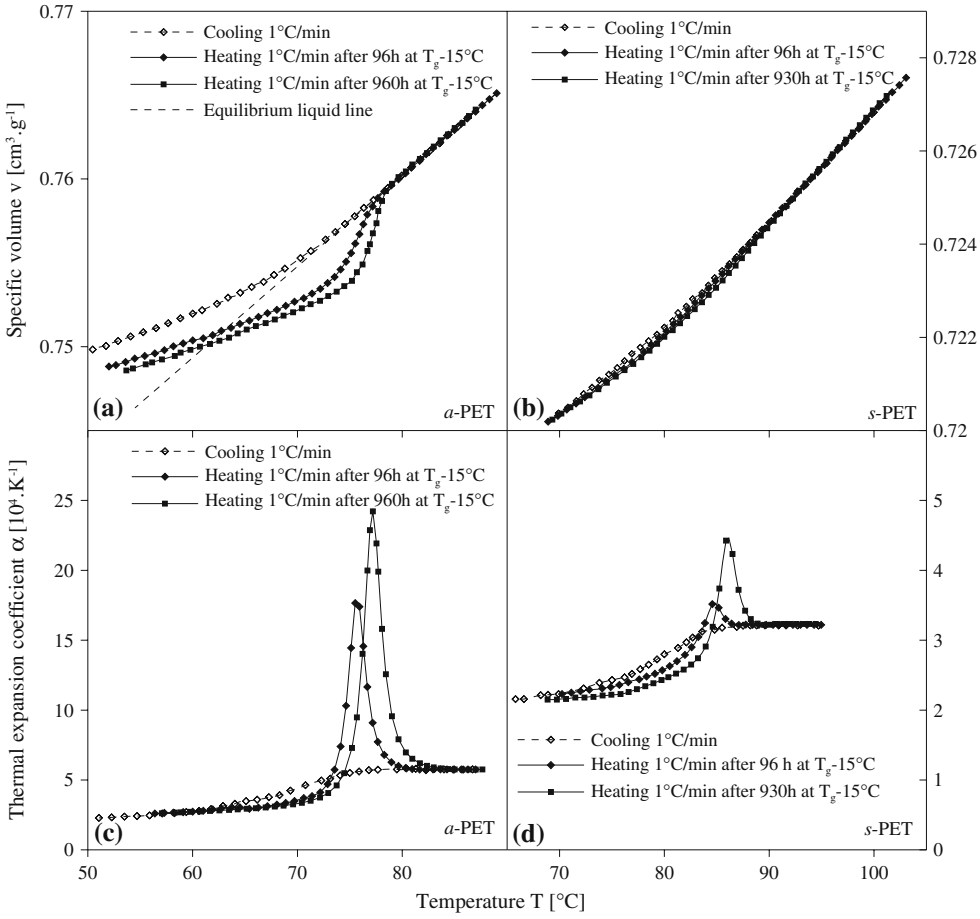

Fig. 3 Volume dilatometry results: (**a**) and (**b**) specific volume changes with temperature under constant heating/cooling rates; (**c**) and (**d**) temperature dependence of thermal expansion coefficient calculated from the above data. Left figures—*a*-PET, right—*s*-PET

Table 1 Thermal properties of *a*-PET and *s*-PET

Calorimetric data					
Material	$T_{g,ent.}$ (°C)	c_{pg} (J g^{-1} K^{-1})	c_{pl} (J g^{-1} K^{-1})	Δc_{pg} (J g^{-1} K^{-1})	x_w (%)
a-PET	69.1	1.24	1.59	0.35	11.8
s-PET	81.5	1.23	1.38	0.15	20.8
Dilatometric data					
Material	$T_{g,vol}$ (°C)	α_l (10^4 K^{-1})	α_g (10^4 K^{-1})	$\Delta\alpha$ (10^4 K^{-1})	x_ϕ (%)
a-PET	67.8	5.55	2.24	3.31	7.5
s-PET	77.5	2.76	1.49	1.27	25.7

cient of amorphous PET, α_{am}, was extrapolated from the dependency of $\Delta\alpha$ for different crystallinity content according Lin et al. [16] and Androsch et al. [17] who reported that the decrease in Δc_p with crystallinity is linear up to 10% of crystalline fraction content. We derived $\Delta\alpha$ for 4.2 and 7.0 wt.% crystallinity samples to be 2.98×10^{-4} K^{-1} and 2.58×10^{-4} K^{-1} which gives together with value for *a*-PET sample 3.31×10^{-4} K^{-1}, $\Delta\alpha_{am} = 3.68 \times 10^{-4}$ K^{-1}. For completeness, T_g increases to 68 and 69.1 °C, respectively. The volumetric value of RAF for *s*-PET 25.7% corresponds to the value of 18% reported by Lin et al. [16] for melt-crystallized PET measured by calorimetry. The values reported for PET samples with similar crystallinity to *a*-PET by Lin et al. [16] and Androsch and Wunderlich [17], achieved almost 0% and 2.3% of RAF, respectively, compared to our 7.5%.

Volume relaxation data are presented in Fig. 4 (*a*-PET) and Fig. 5 (*s*-PET). The contraction isotherms show that general aspects of structural relaxation are kept also during the relaxation of such heterogeneous structures. In both cases of *a*-PET and *s*-PET the typical sigmoidal shape of relaxation isotherms in logarithm of relaxation time can be observed; in the first part an initial plateau is observed, then it starts to decrease faster and nearly linearly going through inflection point, and finally it comes to equilibrium. The relative departure of volume from equilibrium, δ, is defined by Eq. (6) where v_∞ means the volume in equilibrium:

$$\delta = \frac{v_{(t)} - v_\infty}{v_\infty} \tag{6}$$

Its value increases by lowering of relaxation temperature, T_a, together with extending of process time scale. The presence of crystals significantly modifies structural relaxation parameters. It is evident that relative departure is approximately three times smaller in the case of *s*-PET than for *a*-PET, compared data at similar temperatures in relation to T_g. Further the time scales of reaching the equilibrium are approximately one and half times longer for *s*-PET than in the case of *a*-PET. Measured relaxation times-scales of *a*-PET

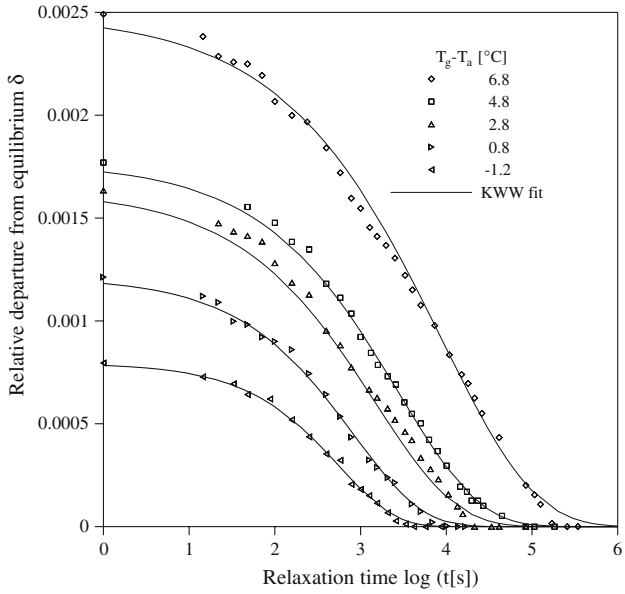

Fig. 4 Volume relaxation isotherms after temperature down-jumps from equilibrium at $T_i = T_g + 10$ °C to different relaxation temperatures, T_a, in glass transition region for *a*-PET

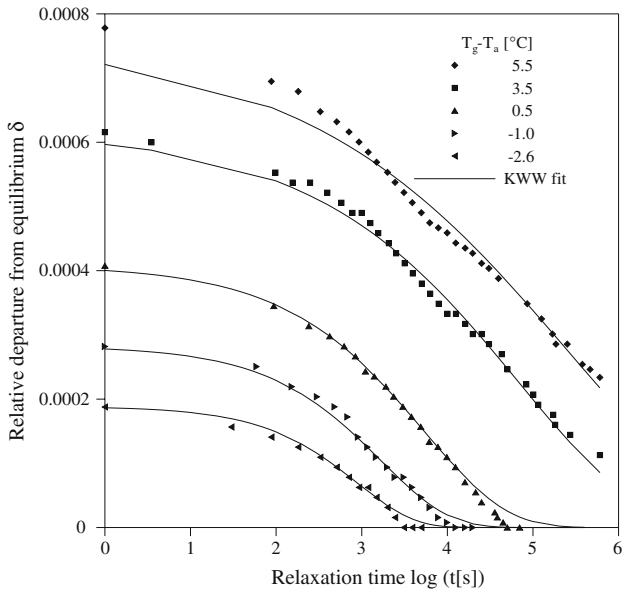

Fig. 5 Volume relaxation isotherms after temperature down-jumps from equilibrium at $T_i = T_g + 10$ °C to different relaxation temperatures, T_a, in glass transition region for *s*-PET

corresponds well to results the amorphous PET measured by Aref-Azar et al. [11], Lu and Hay [28] and are shorter than reported by Itoyama [23,29] for amorphous and low crystalline sample (2.3%). Times scales of *s*-PET are similar to those reported for highly crystallized PET by Aref-Azar et al. [11].

The isothermal aging can be considered an inherently non-exponential process, usually involving the stretched exponential relaxation function associated with the names of Kohlrausch–Williams–Watts (KWW) [2,4,11,30]. KWW equation reads as:

$$\phi(t) = \exp\left[-\left(\frac{t_a}{\tau}\right)^{\beta}\right] \tag{7}$$

where t_a represents time, τ means relaxation time, and β $(0 < \beta < 1)$ is a stretching exponent, a parameter which is a reciprocal measure of the breadth of the relaxation times distribution and $\phi(t)$ represents normalized volume data:

$$\phi(t) = \frac{v_{(t)} - v_\infty}{v_0 - v_\infty} \tag{8}$$

where v_0 is the initial volume. The course of isothermal relaxation calculated by KWW model is presented in Figs. 4 and 5 as solid lines.

Master curve of $\phi(t)$ against $\log(t_a/\tau)$ calculated from the data gives average values of β, 0.48 ± 0.01 for *a*-PET and 0.36 ± 0.02 for *s*-PET. Further, an activation energy of transition from glass to liquid, Δh, can be by calculated from an Arrhenius plot of $\ln(\tau)$ versus reciprocal aging temperature. For *a*-PET the value amounting 407 ± 50 kJ mol^{-1} and for *s*-PET 1012 ± 120 kJ mol^{-1} were achieved. According to this, *s*-PET has a broader distribution of relaxation times and highly cooperative process compared with *a*-PET.

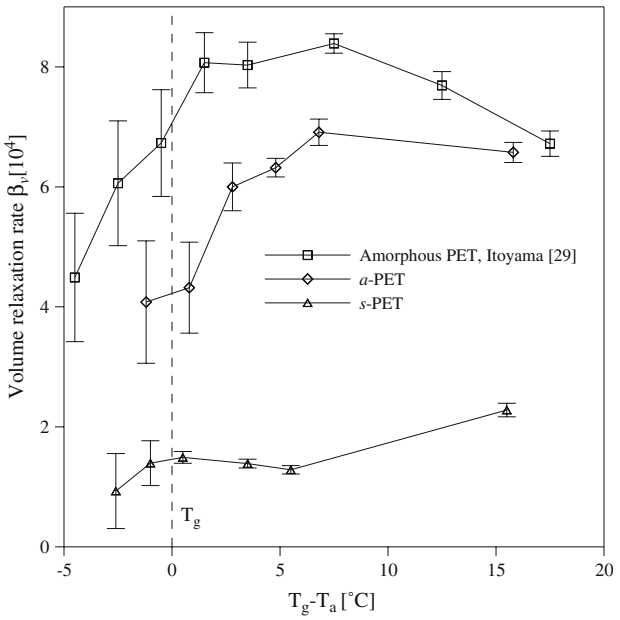

Fig. 6 Volume relaxation rate, β_v, calculated from the data in Figs. 4 and 5. $\beta_v(T)$ of amorphous PET calculated from the data of Itoyama [29]

The volume relaxation process can be quantitatively analyzed using a volume relaxation rate, β_v [2,5,9,10,22,31–33]. It is defined as a slope of the volume contraction isotherms in the region where the specific volume varies linearly with the logarithm of aging time, which can be expressed by the following equation:

$$\beta_v = \left(\frac{d\delta}{d\log t_a}\right)_{inf} \cong -\frac{1}{v}\left(\frac{dv}{d\log t_a}\right)_{inf} \tag{9}$$

where t_a represents relaxation time, and δ again the relative departure of volume from equilibrium.

The calculated values of β_v are presented in Fig. 6 together with error bars (calculated with the help of Student *t* distribution, probability of error $\alpha = 0.0005$). In addition, Fig. 6 also show the data adopted from Itoyama [29] (based on T_g equals 67.5 °C). Moreover, the Fig. 6 demonstrates a reduction of β_v with an increase in crystallinity. A comparison of β_v trend of amorphous PET and *a*-PET also revealed an decreasing discrepancy between both curves with growing distance from T_g. When comparing the calculated values of volume relaxation rates for both materials relaxed at T_g–15 °C one can find decrease of β_v from $7.7 \pm 0.23 \times 10^{-4}$ for amorphous PET to $2.2 \pm 0.12 \times 10^{-4}$ for *s*-PET. This decrease is higher than can be expected from the content of relaxation inert crystals decelerating β_v of about some 47%. Finally, these values can be compared with one from literature where for example Struik [22] reported β_v for amorphous PET 5.8×10^{-4} and 2.1×10^{-4} [9] for the semicrystalline one.

Conclusion

The thermal analysis and volume relaxation measurements were carried out for an amorphous and semicrystalline PET. The presence of crystalline phase resulted in significant changes of thermal properties, such as an increase in T_g, broadening of the transition zone, and decrease in Δc_p and $\Delta\alpha$ in glass transition. The decrease in Δc_p as well as in $\Delta\alpha$ was higher than that predicted based on the sample crystallinity. This phenomenon was attributed to the presence of rigid amorphous fraction at the interface of amorphous

phase and crystals. The amount of rigid amorphous fraction was determined to be about 21–26% for high crystallized PET. Furthermore, the presence of crystalline phase reduced volume relaxation rates. And finally, also other relaxation characteristics such as stretching parameter β from KWW function or activation energy for transition from glass to liquid, Δh, were affected by sample crystallinity indicating a broader distribution of relaxation times of relaxing amorphous phase.

Acknowledgements The financial support of the Ministry of Education, Youth and Sports of the Czech Republic in the frame of project MSM7088352101 is gratefully acknowledged

References

1. Hutchinson JM (1995) Prog Polym Sci 20:703
2. Haward RN, Young RJ (1997) The physics of glassy polymers. Chapman & Hall, London, p 85
3. Slobodian P, Říha P, Lengálová A, Hadač J, Sáha P, Kubát J (2004) J Non-Cryst Solids 344:148
4. Liška M, Chromčíková M (2005) JTAC 81:125
5. Struik LCE (1978) Physical aging of amorphous polymers and other materials. Elsevier, Amsterdam
6. Montserrat S, Cortes P (1995) J Mater Sci 30:1790
7. Vigier G, Tatibouet J (1993) Polymer 34:4257
8. Alves NM, Mano JF, Balaguer E, Meseguer Dueñas JM, Gomez Ribelles JL (2002) Polymer 43:4111
9. Struik LCE (1987) Polymer 28:1521
10. Struik LCE (1987) Polymer 28:1534
11. Aref-Azar A, Arnoux F, Biddlestone F, Hay JN (1996) Thermochim Acta 273:217
12. Fukao K, Miyamoto Y (1997) J Non-Cryst Solids 211:208
13. Vigier G, Tatibouet J, Benatmane A, Vassoille R (1992) Colloid Polym Sci 270:1182
14. Coburn JC, Boyd RH (1986) Macromolecules 19:2238
15. Monserrat S, Colomer P, Belana J (1992) J Mater Chem 2:217
16. Lin J, Shenogin S, Nazarenko S (2002) Polymer 43:4733
17. Androsch R, Wunderlich B (2005) Polymer 46:12556
18. Okazaki I, Wunderlich B (1996) J Polym Sci Polym Symp 34:2941
19. Zhao J, Dong W, Li C, Guo M, Fan Q (2003) Macromolecules 36:2176
20. Tant MR, Wilkes GL (1981) Polym Eng Sci 21:874
21. Mukherjee S, Jabarin SA (1995) Polym Eng Sci 35:1145
22. Struik LCE (1987) Polymer 28:1869
23. Itoyama K (2001) Nihon Reoroji Gakkaishi 29:21
24. Chung HJ, Chang HI, Lim ST (2004) Carbohydr Res 58:101
25. Brandrup J, Immergut EH (1989) Polymer handbook, 3rd edn. John Wiley & Sons Inc., New York, p V/101
26. Grebowicz J, Lau SF, Wunderlich BJ (1984) J Polym Sci Polym Symp 71:19
27. Suzuki H, Grebowicz J, Wunderlich BJ (1985) Macromol Chem 186:1109
28. Lu X, Hay JN (2000) Polymer 41:7427
29. Itoyama K (1999) Nihon Reoroji Gakkaishi 27:25
30. Williams G, Watts DC (1970) Trans Faraday Soc 66:80
31. Greiner R, Schwarzl FR (1984) Rheol Acta 23:378
32. Robertson CG, Wilkes GL (2000) Polymer 41:9191
33. Slobodian P, Lengálová A, Sáha P (2004) Polym J 36:176